Smart Structures and Systems, Vol.11, No. 1 (2013) 103-122
DOI: http://dx.doi.org/10.12989/sss.2013.11.1.103

Particle filter for model updating and reliability estimation of existing structures

Ikumasa Yoshida[*1] and Mitsuyoshi Akiyama[2]

[1]*Department of Civil Engineering, Tokyo City University, Tokyo, 158-8557, Japan*
[2]*Department of Civil Engineering, Waseda University, Sendai, 980-8579, Japan*

(Received June 11, 2012, Revised November 25, 2012, Accepted November 30, 2012)

Abstract. It is essential to update the model with reflecting observation or inspection data for reliability estimation of existing structures. Authors proposed updated reliability analysis by using Particle Filter. We discuss how to apply the proposed method through numerical examples on reinforced concrete structures after verification of the method with hypothetical linear Gaussian problem. Reinforced concrete structures in a marine environment deteriorate with time due to chloride-induced corrosion of reinforcing bars. In the case of existing structures, it is essential to monitor the current condition such as chloride-induced corrosion and to reflect it to rational maintenance with consideration of the uncertainty. In this context, updated reliability estimation of a structure provides useful information for the rational decision. Accuracy estimation is also one of the important issues when Monte Carlo approach such as Particle Filter is adopted. Especially Particle Filter approach has a problem known as degeneracy. Effective sample size is introduced to predict the covariance of variance of limit state exceeding probabilities calculated by Particle Filter. Its validity is shown by the numerical experiments.

Keywords: conditional reliability; update; failure probability; Particle Filter ;Bayesian

1. Introduction

Some model parameters are often difficult to determine in advance, or uncertainties of the parameters increase over time. The model parameters should be updated by inspection data or observation data in order to estimate current condition of existing structures properly. This paper proposes updating of reliability estimation of existing structures. It is composed of two parts, update of the model by observation or inspection data and estimation of limit state exceeding probability based on the updated model. The uncertainties of model parameters should be decreased depending on the quantity and quality of the observation/inspection data. Consequently more credible information can be provided for reasonable decision-making. Updating of model parameters is referred by several terminologies, such as parameter identification, inversion, back analysis, data assimilation and so on. Parameter updating or identification of a model is one of the hottest topics that have attracted attention from many researchers for decades (e.g., Yun and Shinozuka 1980, Hoshiya and Saito 1983, Honjo *et al*. 1994, Ge and Soong 1998, Au 2011). Only

*Corresponding author, Professor, E-mail: iyoshida@tcu.ac.jp

representative value of the model parameters is often focused, but probabilistic nature of an updated model is important when we discuss update of limit state probabilities. The difficulties in obtaining solution in Bayesian updating depend on non-linearity of related equation and non-Gaussian PDFs of model parameters. In problems in which all equations are linear and all random variables are modelled by Gaussian, a closed form solution exists. They are known as Kalman filter algorithm in time domain or Kriging in spatial domain (Hoshiya and Yoshida 1996, Hoshiya and Yoshida 1998).

When nonlinearity or non-Gaussian model parameters are involved, a rigorous theoretical approach is generally impossible to implement in realistic cases. An approximate solution can, however, be found by using several approaches. An idea of Gaussian sum is one of the approaches (Alspach *et al*. 1972). Weighted sum of Gaussian PDF (probability density function) is used to approximate arbitrary form of PDF. This is a good way to handle the nonlinear and non-Gaussian problem, but it has serious difficulty like numerical integration when the number of parameter is large. Several ideas are proposed to handle non-linear/non-Gaussian problems but most of them end up with same problem, so-called curse of dimensionality. Monte Carlo (MC) approach is in general used because of its versatility and usefulness to large dimension problem. Though an early idea of MC based methods for non-linear filtering technique can be found in late 1960s, the methods have been developed since 1990s intensively. MC based methods include Particle Filter, MC filter, Bootstrap filter, recursive MCS, sequential MCS, the Sampling Importance Resampling (SIR) method, and the Sequential Importance Sampling with Resampling (SISR) (Gordon *et al*. 1993, Kitagawa 1996, Arulampalam *et al*. 2002, Ristic *et al*. 2004). In this paper, the term Particle Filter (PF) is used in conjunction with time-dependent reliability assessment. Many researchers in various fields such as space physics, geophysics and medical science use PF to identify model parameters. Though they sometimes use a term, data assimilation instead of parameter identification, it is basically used in same meaning. An application of the PF for identification of structural model parameter is found also in civil engineering (Sato and Kaji 2002, Yoshida and Sato 2002). Ensemble Kalman filter (Evensen 1994) or unscented Kalman filter (Julier and Uhlmann 1997) are also developed to treat problems with nonlinearity. They are good

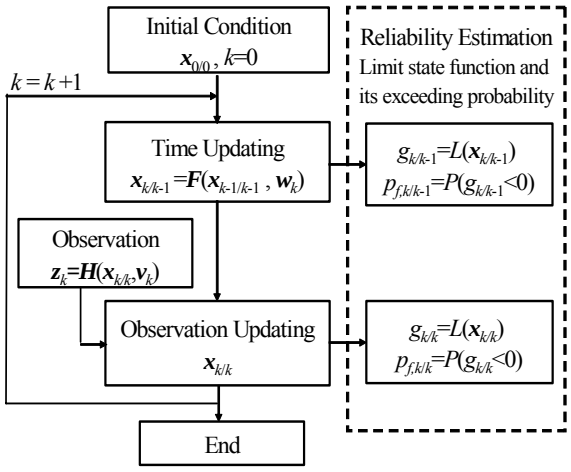

Fig. 1 Reliability estimation with update

methods to estimate representative value. Their calculation cost is lower than that of PF. When limit state probability is concerned, however we cannot expect enough accuracy because they ignore 3rd moment or higher, which sometimes have significant influence on tail part of PDF, consequently limit state probability.

Authors proposed updated reliability analysis by using Particle Filter (Yoshida *et al*. 2009, Akiyama *et al*. 2010). We discuss how to apply the proposed method through numerical examples on reinforced concrete (RC) structures after verification of the method with hypothetical linear Gaussian problem. Reinforced concrete (RC) structures in a marine environment deteriorate with time due to chloride-induced corrosion of reinforcing bars. In the case of existing structures, it is essential to monitor the current condition and to reflect it to rational maintenance with consideration of the uncertainty. In this context, updated reliability estimation of a structure provides useful information for the rational decision.

2. Formulation of reliability analysis with update

State space model consists of two processes, time updating process and observation updating process. The time updating process is the one step ahead prediction based on the information at (k-1)-th step. The predicted state vector is

$$x_{k/k\text{-}1} = F(x_{k-1/k-1}, w_k) \tag{1}$$

where $\boldsymbol{w}_k$ is system noise that is involved in the prediction process including modelling error effects or unforeseen disturbances. State vector $\boldsymbol{x}_{k\text{-}1/k\text{-}1}$ is model parameters with uncertainties at (k-1)-th step, which is updated reflecting observation data up to (k-1)-th step. It is assumed that observation information $\boldsymbol{z}_k$ is a function of state vector $\boldsymbol{x}_{k/k}$ and observation noise $\boldsymbol{v}_k$ as

$$z_k = H(x_{k/k}, v_k) \tag{2}$$

The PDF (Probability Density Function) of these noises, $p(\boldsymbol{w}_k)$ and $p(\boldsymbol{v}_k)$ are assumed known and independent. Updating of state vector $\boldsymbol{x}_{k/k}$ from $\boldsymbol{x}_{k/k\text{-}1}$ with $\boldsymbol{z}_k$ is called observation updating process. When the state and observation equations are linear and noises are Gaussian, Kalman filter algorithm provides exact solution. The real world problems, however, often involve nonlinearity and non-Gaussian noises.

The filtering algorithm based on MCS attracted attention for nonlinear and/or non-Gaussian problems. Fig. 1 shows the outline of the algorithm. It starts by assuming samples drawn from the distribution at (k-1)-th step

$$x_{k-1/k-1}^{(j)} \sim p(x_{k-1}|Z_{k-1}), \qquad j = 1,\cdots,n \tag{3}$$

$$Z_{k-1} = (z_1, z_2, \cdots, z_{k-1}) \tag{4}$$

The superscript (j) denotes the generated j-th sample realization. Cumulative distribution $P(x_{k-1}|Z_{k-1})$ can be naturally expressed approximately by the generated samples.

$$P(x_{k-1}|Z_{k-1}) \cong \frac{1}{n}\sum_{j=1}^{n} U(x_{k-1} - x_{k-1/k-1}^{(j)}) \tag{5}$$

where U is step function. The approximate PDF is obtained by differentiation with respect to $\boldsymbol{x}$.

$$p(x_{k-1}|Z_{k-1}) \cong \frac{1}{n}\sum_{j=1}^{n}\delta(x_{k-1} - x_{k-1/k-1}^{(j)}) \tag{6}$$

where δ denotes Dirac delta function which is derivative of step function U. This approximation form of PDF with sample realizations is called as empirical PDF. The samples of k-th step before observation updating are obtained by simply substituting the samples into Eq. (1)

$$x_{k/k-1}^{(j)} = F(x_{k-1/k-1}^{(j)}, w_k^{(j)}) \tag{7}$$

The empirical PDF of k-th step before updating is similarly estimated by the sample realization

$$p(x_k|Z_{k-1}) \cong \frac{1}{n}\sum_{j=1}^{n}\delta(x_k - x_{k/k-1}^{(j)}) \tag{8}$$

The PDF after updating is obtained by using Bayesian theorem.

$$p(x_k|Z_k) = p(x_k|z_k,Z_{k-1}) = \frac{p(x_k,z_k|Z_{k-1})}{p(z_k|Z_{k-1})} = \frac{p(z_k|x_k,Z_{k-1})p(x_k|Z_{k-1})}{\int p(z_k|x_k,Z_{k-1})p(x_k|Z_{k-1})dx_k} \tag{9}$$

Substituting Eq. (8) into Eq. (9), we have

$$p(x_k|Z_k) = \frac{p(z_k|x_k,Z_{k-1})\frac{1}{n}\sum_{j=1}^{n}\delta(x_k - x_{k/k-1}{}^{(j)})}{\int p(z_k|x_k,Z_{k-1})\frac{1}{n}\sum_{j=1}^{n}\delta(x_k - x_{k/k-1}{}^{(j)})dx_k} \tag{10}$$

Eq. (10) can be integrated by using the nature of a delta function.

$$p(x_k|Z_k) = \sum_{j=1}^{n}\left(\frac{q_k^{(j)}}{\sum_{i=1}^{n}q_k^{(i)}}\right)\delta(x_k - x_{k/k-1}{}^{(j)}) = \sum_{j=1}^{n}a_k{}^{(j)}\delta(x_k - x_{k/k-1}{}^{(j)}) \tag{11}$$

where

$$a_k^{(j)} = \frac{q_k^{(j)}}{\sum_{i=1}^{n}q_k^{(i)}} \tag{12}$$

$$q_k{}^{(j)} = p(z_k|x_{k/k-1}{}^{(j)}) \tag{13}$$

The term $a_k^{(j)}$ represents weight (likelihood ratio) of sample j after updating.

When a new observation is available, the weights are calculated again and the approximate posterior PDF is sequentially updated. However after a few steps the confidence in the estimated PDF sometimes deteriorates because many particles have normalized weights very close to zero. This phenomenon is called as weight degeneracy or sample impoverishment. To alleviate the sample impoverishment problem, a resampling step is introduced (Arulampalam *et al*. 2002, Ristic *et al*. 2004). A new set of samples $\mathbf{x}_{k/k}^{(j)}$, j=1, n. is obtained by resampling independently n samples from $\mathbf{x}_{k/k-1}^{(j)}$ proportional to the weight $a_k^{(j)}$. The set of sample realization approximates updated PDF $p(x_k|Z_k)$.

$$p(x_k|Z_k) \cong \frac{1}{n}\sum_{j=1}^{n}\delta(x_k - x_{k/k}^{(j)}) \tag{14}$$

A limit state function g is given as a function of state vector $\boldsymbol{x}$.

$$g = L(x) \tag{15}$$

A limit state exceeding probability can be calculated easily with the samples updated by up to k-th step observation data Z_k.

$$p_{f,k/k} = p(g<0) = 1 - \frac{1}{n}\sum_{j=1}^{n} U\left(g\left(x_{k/k}{}^{(j)}\right)\right) \tag{16}$$

The procedure can be summarized as follows corresponding to Fig. 1,

(a) Generate sample realization based on the initial PDF, $x_{0/0}{}^{(j)}$, $j = 1, n$
(b) Perform time updating process with Eq. (7)
(c) Calculate weight (likelihood) of each sample with Eqs. (12) and (13) based on given observation data
(d) Re-sample according to normalized likelihood (weight)
(e) Go to step (b)

3. Verification with hypothetical linear Gaussian Model

3.1 Limit state function and basic conditions

Limit state exceeding probabilities can be obtained theoretically when limit state function, state equation and observation equation are linear and all related noises are modelled by Gaussian. In this section, validity of reliability estimation with PF is shown with a simple linear Gaussian problem through comparison with probabilities calculated theoretically.

Hypothetical limit state function g is defined as

$$g_{k/k} = Lx_{k/k} = (x_{1,k/k} - x_{2,k/k} \times t) - x_{3,k/k} \tag{17}$$

where,

$$x_{k/k}{}^{T} = (x_{1,k/k} \quad x_{2,k/k} \quad x_{3,k/k}), \quad L = (1 \quad -t \quad -1) \tag{18}$$

where t is years after construction, $x_{1,\,k/k}$, $x_{2,\,k/k}$, $x_{3,\,k/k}$ are state variables (random variables)

involved in the limit state function, which are assumed to be independent and Gaussian. Subscript k stands for step number. It is noted that a vector $\boldsymbol{x}_{k/k}$ is expressed in a bold font, while a component of vector $x_{1,k/k}$, $x_{2,k/k}$ and $x_{3,k/k}$ are expressed in normal font. These random variables and the limit state function are hypothetical, and do not have any physical meaning, however, resistance R and action S are defined as follows for illustrative purpose.

$$R_{k/k} = x_{1,k/k} - x_{2,k/k} \times t, \qquad S_{k/k} = x_{3,k/k} \tag{19}$$

State equation is assumed to be stationary

$$x_{k/k} = x_{k/k-1} + w_k \tag{20}$$

where noise w in a state equation is process noise which is also assumed to be independent and Gaussian. Assumed mean and variance are summarized in Table 1. Variances of process noise w_2, w_3 are 0.0, and that of w_1 is 2.0, which represents increase of uncertainty as to x_1 over time, 20 years in this numerical example.

Limit state value g is also Gaussian since noises are Gaussian and limit state function is linear. The limit state probability can be calculated easily when observation update is not considered. Mean and variance of g, and limit state probabilities just after the construction (t = 0) and at 20 years after the construction (t = 20) are summarized in Table 2.

3.2 Probabilities updated theoretically

We assume the following hypothetical observation equation.

$$z_k = Hx_{k/k} + v = (1 \quad -2t \quad 0)\begin{pmatrix} x_{1,k/k} \\ x_{2,k/k} \\ x_{3,k/k} \end{pmatrix} + v \tag{21}$$

where v is observation noise which is assumed to be independent and Gaussian, of which variance is assumed to be 1.0. Let's assume that observation data z is given at 20 years after construction. k = 0 means just after the construction, k = 1 means 20 years after construction in this numerical

Table 1 Statistics of random variables

	$x_{0/0.,1}$	$x_{0/0.,2}$	$x_{0/0.,3}$	$w_{1,1}$	$w_{1,2}$, $w_{1,3}$
Mean	15.0	0.1	10.0	0.0	0.0
Variance	1.0	0.01	4.0	2.0	0.0

w_1 shows 20 years variance

Table 2 Statistics of limit state value g and limit state probabilities

Year	Mean	Variance	Reliability index	Probability
0	5	5	2.24	0.013
20	3	11	0.90	0.18

β: Reliability Index

example. Because all involved uncertainties are modelled by Gaussian and observation equation is also linear, PDF of the random variables can be updated theoretically. Please refer a textbook on Kalman filter or Hoshiya and Yoshida (1996) for more detail.

Three cases of observation data $z_1 = 8, 11, 13$ are assumed. If z at 20 years is calculated simply by the mean value shown in Table.1, we have $z_1 = 11$ by Eq. (21). Therefore the three cases of observation $z_1 = 8, 11, 13$ indicate bad, average, safe side for the limit state respectively. The limit state probabilities are calculated based on the state vector $\boldsymbol{x}$ updated by the observations.

The covariance matrices of random variables before update are

$$P_{0/0} = \begin{pmatrix} 1 & 0 & 0 \\ 0 & 0.01 & 0 \\ 0 & 0 & 4 \end{pmatrix}, \quad P_{1/0} = \begin{pmatrix} 3 & 0 & 0 \\ 0 & 0.01 & 0 \\ 0 & 0 & 4 \end{pmatrix} \tag{22}$$

$\boldsymbol{P}_{0/0}$ represents covariance matrix of state vector just after construction ($t = 0$). $\boldsymbol{P}_{1/0}$ represents covariance matrix at 20 years ($t = 20$) before observation updating. The covariance matrix after update $\boldsymbol{P}_{1/1}$ is

$$P_{1/1} = (H^T R^{-1} H + P_{1/0}^{-1})^{-1} = \left[\begin{pmatrix} 1 \\ -40 \\ 0 \end{pmatrix} \begin{pmatrix} 1 & -40 & 0 \end{pmatrix} + \begin{pmatrix} \frac{1}{3} & 0 & 0 \\ 0 & 100 & 0 \\ 0 & 0 & \frac{1}{4} \end{pmatrix} \right]^{-1} = \frac{1}{500} \begin{pmatrix} 1275 & 30 & 0 \\ 30 & 1 & 0 \\ 0 & 0 & 2000 \end{pmatrix} \tag{23}$$

where $\boldsymbol{R}$ is covariance matrix of observation error. It does not appear in right hand side of the equation, because it is 1×1 matrix and its variance is 1.0. When $z_1 = 11$, mean of random variables are updated as follows.

$$\begin{aligned} \bar{x}_{1/1} = \bar{x}_{1/0} + P_{1/1} H^T R^{-1} (z_1 - H\bar{x}_{1/0}) &= \begin{pmatrix} 15 \\ 0.1 \\ 10 \end{pmatrix} + \frac{1}{500} \begin{pmatrix} 1275 & 30 & 0 \\ 30 & 1 & 0 \\ 0 & 0 & 2000 \end{pmatrix} \begin{pmatrix} 1 \\ -40 \\ 0 \end{pmatrix} (11\text{-}15+4) \\ &= \begin{pmatrix} 15 \\ 0.1 \\ 10 \end{pmatrix} + \frac{1}{500} \begin{pmatrix} 75 \\ -10 \\ 0 \end{pmatrix} \times 0 = \begin{pmatrix} 15 \\ 0.1 \\ 10 \end{pmatrix} \end{aligned} \tag{24}$$

In a linear Gaussian problem, updated variables are also Gaussian. Consequently the limit state function value $g_{1/1}$ is Gaussian because the limit state function is also linear. Its mean E $[g_{1/1}]$ and variance Var $[g_{1/1}]$ are obtained easily.

$$E[g_{1/1}] = E[Lx_{1/1}] = 3.0 \tag{25}$$

$$\mathrm{Var}[g_{1/1}] = LP_{1/1}L^T = 4.95 \tag{26}$$

From above information, limit state probability $P(g_{1/1} < 0)$ is 0.089. In the same way, when $z_1 = 8, 13$, limit state probabilities are 0.27, 0.033 respectively.

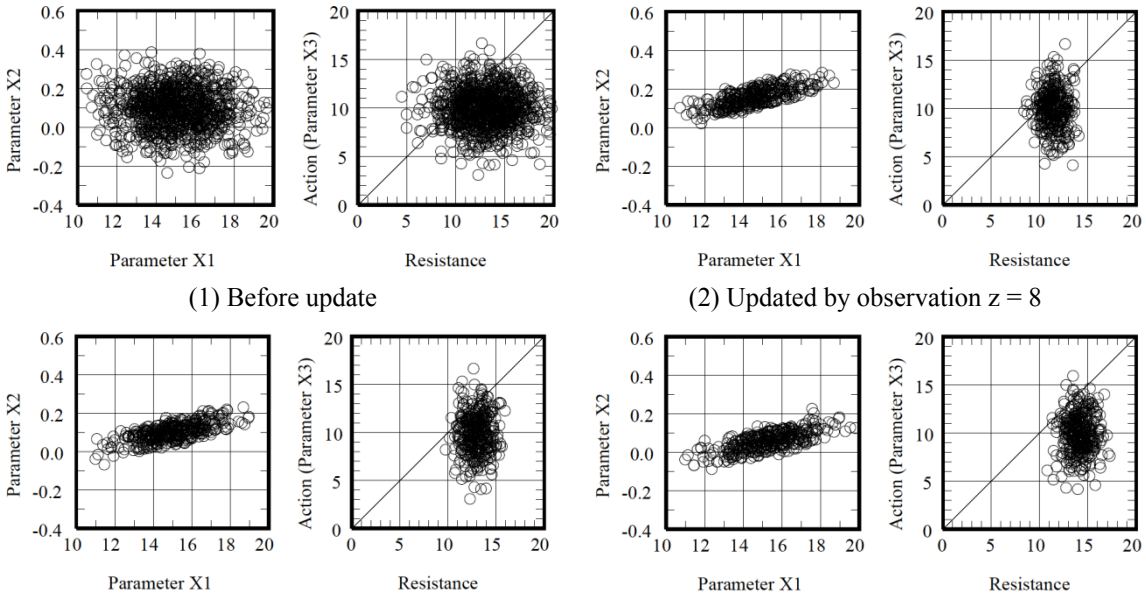

(1) Before update (2) Updated by observation z = 8

(3) Updated by observation z = 11 (4) Updated by observation z = 13

Fig. 2 Sample realizations for hypothetical problem by particle filter

3.3 Probabilities updated by Particle Filter (PF)

The same problem is solved by using PF following the procedure stated in Chap. 2. In step (a), sample realization $\boldsymbol{x}_{0/0}^{(j)}$ are generated according to the statistics in Table 1. In step (b), $\boldsymbol{x}_{1/0}^{(j)}$ is obtained by simply adding the process noise, because time update process is stationary as shown in Eq. (20). In step (c), likelihood of sample realization j is calculated with $\boldsymbol{x}_{1/0}^{(j)}$ as follows, because the observation noise is modelled by Gaussian distribution.

$$q_1^{(j)} = c_a \exp\left(-\frac{\left(z_1 - x_{1,1/0}^{(j)} - 2t x_{2,1/0}^{(j)}\right)^2}{2\sigma_v^{\,2}} \right), \text{ where, } \quad c_a = \frac{1}{\sqrt{2\pi}\sigma_v}, t = 20, \sigma_v = 1.0 \tag{27}$$

where σ_v is standard deviation of observation noise. Normalized likelihood, namely weight $a_1^{(j)}$ is obtained by using Eq. (12). Finally, $\boldsymbol{x}_{1/1}^{(j)}$ is re-sampled according to weigh $a_1^{(j)}$.

Sample realizations of $\boldsymbol{x}_{1/0}^{(j)}$ are shown in Fig. 2 with sample size 1000. Fig. 2 (a) indicates two kinds of figure at 20 years before update. One is a distribution of samples in $x_{1,1/0}$ and $x_{2,1/0}$ space. The other is the distribution in resistance R and action S space, which are defined in Eq. (19). The samples above the diagonal line shown in the figure exceed the limit state. From the number of the limit state exceeding samples, limit state probability can be calculated easily. The procedure so far is same as ordinary MCS procedure.

Figs. 2(b), (c) and (d) show sample realizations after observation update by z = 8, 11 and 13 respectively. In Fig. 2(b), because observation $z_1 = 8$ (dangerous side, namely highly deteriorated condition) is given, mean and variance of updated resistance is reduced, the limit state probability becomes large from the balance of both. Fig. 2(c) shows the results when observation data $z_1 = 11$

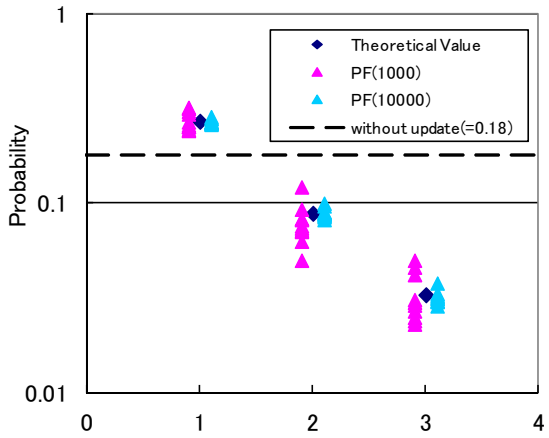

Fig. 3 Updated probabilities by particle filter

(average state) is given. Mean of updated resistance R seems not to be changed but its variance is decreased. Thus samples in limit state exceeding area is decreased, consequently the limit state probability becomes small. Fig. 2(c) indicates the case when observation $z_1 = 13$ (safe side, namely less deteriorated condition) is given. Mean of updated resistance is increased, and its variance is reduced. Consequently the limit state probability becomes small.

Since MCS based methods use random number, probabilities obtained by PF depends on a seed of random number. In order to examine the accuracy of the estimated probabilities, the simulation by PF with a different seed is performed ten times. Sample size of each simulation is 1000 or 10000. Obtained limit state probabilities are shown in Fig. 3 with theoretical probabilities 0.27, 0.089 and 0.033 for $z_1 = 8$, 11 and 13 respectively, which are stated above. When the sample size is 1000, the variance is naturally large compared with cases with 10000 samples, but obtained probabilities are plotted around the theoretical value, which means that unbiased solutions are obtained. Thus we can confirm the validity of conditional reliability estimation with PF. It is noted that strong correlation between $x_{1,\,1/1}$ and $x_{2,\,1/1}$ is observed. From the standpoint of inverse problem, it is impossible to determine the two parameters from one observation data, namely so-called underdetermined problem. However, in terms of updated reliability estimation, the few observation data is still useful to update probabilities.

4. Application to RC Structure in a marine environment

4.1 Limit state functions of RC structure

Reinforced concrete (RC) structures in a marine environment deteriorate with time due to chloride-induced corrosion of reinforcing bars. Because of the presence of uncertainties, it is necessary that structural long-term performance be treated based on reliability concepts and methods (Ellingwood 2005, Frangopol 2009). Three limit state functions are introduced as to deterioration of RC structure due to chloride attack. All uncertainties are denoted by x, which are summarized in Table 3. Please refer Akiyama *et al*. (2010) for more detail.

(1) Limit State 1: Corrosion initiation of rebar, g_1

The limit state for rebar corrosion can be defined using the equation g_1.

$$g_1 = x_7 C_T - C(c, C_0, D_c, t) \tag{28}$$

where

$$C = x_6 C_0 \left(1 - erf \frac{0.1(c + x_5)}{2\sqrt{D_c t}}\right) \tag{29}$$

C_T is the critical threshold value of chloride concentration for initiation of rebar corrosion, x_7 is a random variable representing uncertainty associated with estimation of C_T, C is chloride concentration at rebar (kg/mm^3), C_0 is chloride concentration at concrete surface, x_6 is a random variable related to estimation of C, D_c is apparent diffusion coefficient (cm^2/year), t is the time after construction (year), c is concrete cover specified in design (mm), x_5 is a random variable representing construction error of cover c, erf is error function. C_0 and D_c are given by

$$C_0 = x_4 0.988 C_{air}^{0.379} \tag{30}$$

$$D_c = x_3 10^q, q = -6.77(W/C)^2 + 10.10(W/C) - 3.14 \tag{31}$$

where, x_4 is a random variable representing uncertainty related to estimation C_0, C_{air} is airborne chlorides (mdd), x_3 is a random variable representing uncertainty associated with estimation of D_c, W/C is water cement ratio (%). C_{air} is estimated by the following attenuation equation with respect to the ratio of sea wind r (the breezing time ratio of sea wind), the average wind speed u (m/sec), and a distance from coastline d (m).

$$C_{air} = x_2 1.29 r (x_1 u)^{0.386} d^{-0.952} \tag{32}$$

where, x_2 is a random variable representing model uncertainty of attenuation relationship. All involved uncertainties x_1 to x_7 are summarized in Table 3.

(2) Limit State 2: Corrosion crack occurrence, g_2

The limit state g_2 is defined as

$$g_2 = R_{W2} - S_W \tag{33}$$

where, R_{W2} is the critical threshold of corrosion associated with crack initiation, S_W is corrosion rate (%). R_{W2} is estimated from corrosion quantity W_c (mg/mm^2).

$$W_c = x_8 \frac{\rho_s}{\pi(\gamma - 1)} \times \left(\alpha_0 \beta_0 \frac{0.22\left(\{2(c + x_5) + \phi\}^2 + \phi^2\right)}{E_c(c + x_5 + \phi)} f_c'^{2/3} + \alpha_1 \beta_1 \frac{c + x_5 + \phi}{5(c + x_5) + 3\phi} w_{cr} \right) \tag{34}$$

where, x_8 is a random variable related to the estimation of W_c, ρ_s is iron density (=7.85 mg/mm^3), γ is expansion rate due to corrosion (=3.0), ϕ is diameter of rebar (mm), f_c' is concrete compressive strength (N/mm^2), E_c is concrete stiffness (N/mm^2), w_{cr} is crack width. $\alpha_0, \beta_0, \alpha_1, \beta_1$ are coefficients in order to consider the effect of cover, iron diameter and concrete compressive strength.

$$\begin{aligned}
\alpha_0 &= (-0.0005\phi + 0.028)(c + x_5) + (-0.0292\phi + 1.27) \\
\beta_0 &= -0.0055 f_c' + 1.07 \\
\alpha_1 &= (0.0007\phi - 0.04)(c + x_5) + (0.0663\phi + 5.92) \\
\beta_1 &= -0.0016 f_c' + 1.04
\end{aligned} \tag{35}$$

Action side of iron corrosion rate S_W is estimated as follows.

$$S_W = \begin{cases} 0, & t_1 > t \\ (t - t_1) v_1 x_9, & t_2 > t > t_1 \\ (t_2 - t_1) v_1 x_9 + (t - t_2) v_2 x_9, & t > t_2 \end{cases} \tag{36}$$

$$t_1 = \frac{1}{4 D_c} \left\{ \frac{0.1(c + x_5)}{erf^{-1}\left(1 - \frac{x_7 C_T}{x_6 C_0}\right)} \right\}^2 \tag{37}$$

$$t_2 = t_1 + \frac{R_{W2}}{v_1 x_9} \tag{38}$$

where, v_1 and v_2 are corrosion velocities before and after crack initiation, x_9 a random variable related to the corrosion velocities. The velocities v_1, v_2 are assumed to have following relation.

$$v_2 = \alpha_V v_1 \tag{39}$$

The coefficient α_V is assumed to be 13.0, based on the experimental data.

(3) Limit State 3: Degradation of member strength, g_3

It is assumed that when the corrosion rate reaches 20% (= R_{W3}), the member strength is degraded significantly for numerical demonstration. This third limit state is simply defined by iron corrosion rate S_W and the critical threshold value R_{W3} (= 20%)

$$g_3 = R_{W3} - S_W \tag{40}$$

4.2 Modeling of observation data

The deterioration of reinforced concrete members in important structures such as marine structures, bridges and high-rise towers is routinely monitored using a variety of inspection techniques, ranging from visual inspection, surface sounding, coring for chloride profiling. Visual inspection is most common practice among them. This type of inspection generally gives a rank (category) of deterioration as output. Deterioration rank by visual inspection and profiling of chloride concentrations through depth by coring test are formulated as observation equation in this study.

Visual inspections generally check length and width of crack on concrete surface, grade of surface damage, rust fluid and so on. Among these information, crack width and length are relatively easy to quantify, and have clearer relation with corrosion rate of rebar. In the following numerical simulations, Table 4 is used as the model that shows the relation between deterioration

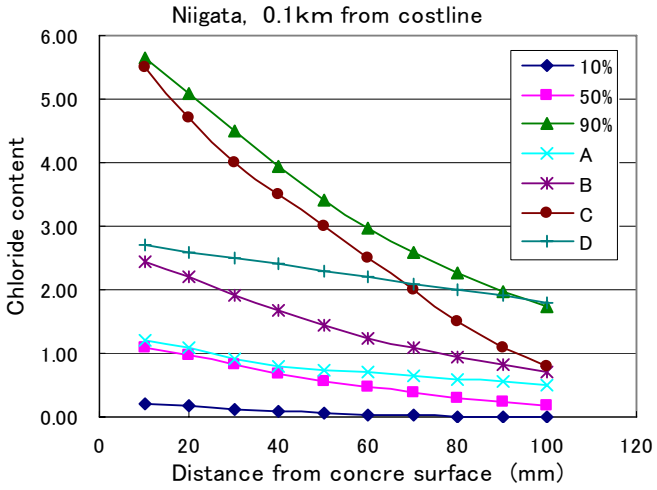

Fig. 4 Distribution of chloride content

rank by visual inspection and corrosion rate of rebar. The rank is assumed to be classified into four states following inspection practice in Japan. Corrosion rate of rebar of rank 1, 2, 3 and 4 are less than 2.3%, 2.3 to 5%, 5 to 20%, larger than 20% respectively. The corresponding boundary values with respect to crack widths are 0.1, 0.2 and 0.5mm, for each rank. Since we assume discrete rank by visual inspection, the observation equation has to be given in the form of table. Each column in Table 4 denotes ranking by visual inspection, namely rank based on crack width, while each line denotes rank based on corrosion rate. In the process of observation update in PF, we need to calculate likelihood of every sample depending on given observation data. The likelihood can be obtained for each sample realization by Table 4 based on rank given by visual inspection. For example, if the visual inspection result (observation data) is III and corrosion rate of a sample is 4% which is categorized in rank II, the likelihood of the sample is 0.313. In the same way, a sample with 1% corrosion rate has likelihood 0.031. An exceptional rule is applied to a sample with 0 % corrosion. Its likelihood is 0.0 when observation is II, III or IV because corrosion crack never occur unless corrosion initiates.

When profiling of chloride concentrations through depth by coring test is given, the observation equation is

$$z = x_6 x_4 0.988 C_{air}^{\ 0.379} \left\{ 1 - erf \frac{0.1d}{2\sqrt{D_c t}} \right\} + v \tag{41}$$

where z is observed chloride concentration at depth of d, v is observation noise. Other notations are same as mentioned earlier.

4.3 Numerical examples of updated reliability estimation

4.3.1 Basic conditions and observation scenario

It is shown how the proposed method can be used to predict stochastic deterioration relating to the long-term chloride corrosion in a reinforced concrete bridge pier. It is assumed that the bridge

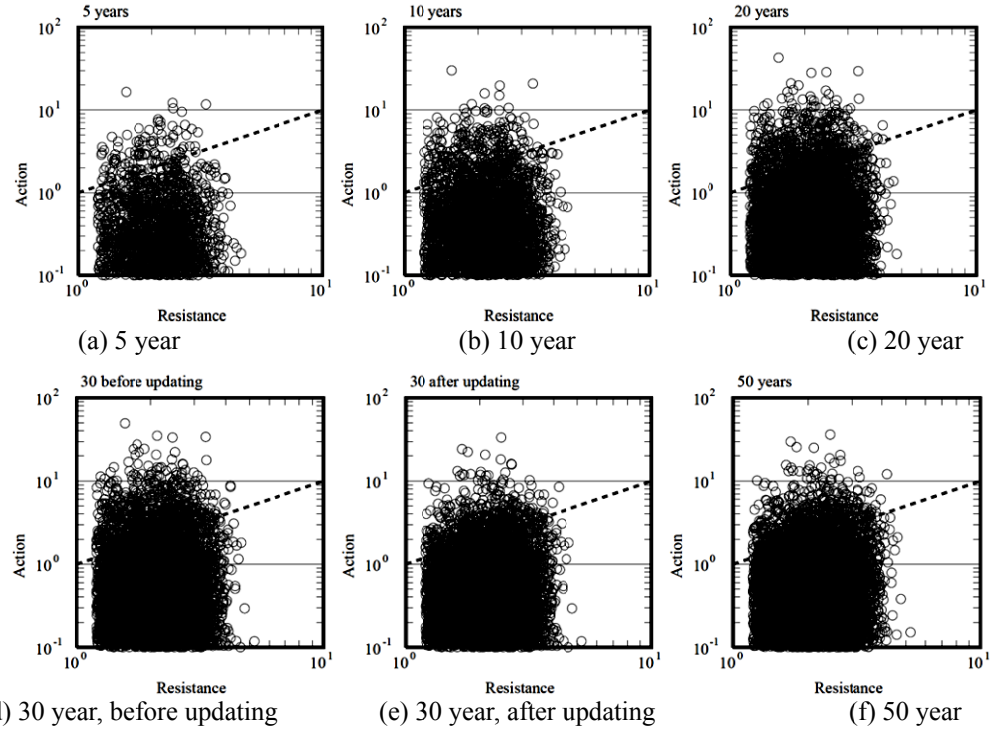

(a) 5 year (b) 10 year (c) 20 year

(d) 30 year, before updating (e) 30 year, after updating (f) 50 year

Fig. 5 Limit state 1, distribution of action and resistance sample realizations, case 1 (visual inspection I)

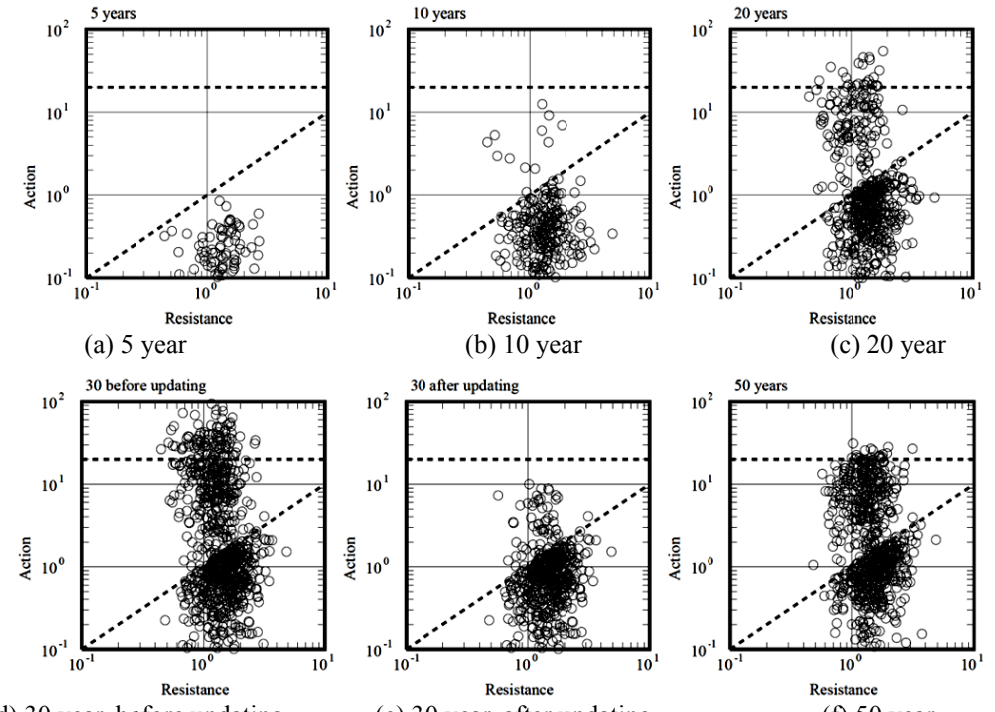

(a) 5 year (b) 10 year (c) 20 year

(d) 30 year, before updating (e) 30 year, after updating (f) 50 year

Fig. 6 Limit state 2, 3, distribution of action and resistance sample realizations, case 1 (visual inspection I)

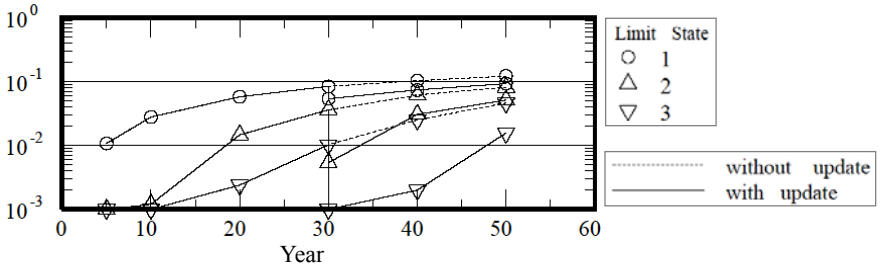

(1) Case 1 (visual inspection I)

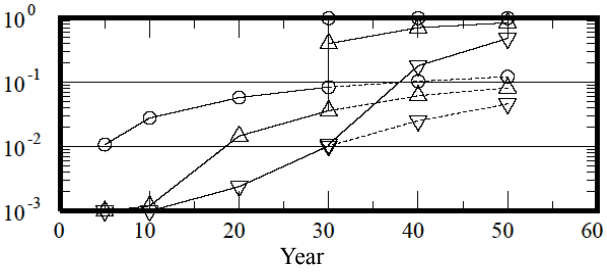

(2) Case 2 (visual inspection II)

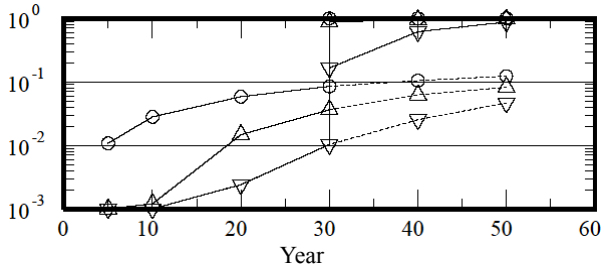

(3) Case 3 (visual inspection III)

Fig. 7 Three kinds of limit state probabilities over time

Table 5 Scenario of observation data set

Case	Years after construction	Observation data	
		Chloride profile	Visual inspection
1	30	-	I
2	30	-	II
3	30	-	III
4	30	B	II
5	30	C	II
6	30	D	II

locates near coastline in Niigata city of Japan. Basic conditions such as water cement ratio and concrete cover are summarized in Table 5.

The assumed profiling data A to D for observation data are shown in Fig. 4, in which 10, 50, 90% lines are percentile of chloride concentration obtained by ordinary MCS with given random variable information in Table 3. Referring those percentile values, observation profiling A, B, C

and D are assumed. Chloride contents at 10, 30, 50, 70 90 mm from concrete surface are used as observation data for illustrative examples by PF. Observation noise v in Eq. (41) is assumed to be 1.0 and independent each other for the simplicity.

Six cases of observation scenario are shown in Table 6. Three kinds of limit state probabilities described in section 4.1 are calculated from 5 years to 50 years after construction by PF with 10000 samples.

4.3.2 Limit state probabilities updated by PF

Sample realizations of action and resistance of the limit state 1 are shown in Fig. 5. They are chloride concentration at rebar as shown in Eq. (28). The broken line in the figure indicates the limit state line for the initiation of rebar corrosion. Samples above the line exceed the limit state, namely indicate initiation of rebar corrosion. The chloride contents become large over time, 5, 10, 20, 30 years, consequently the number of samples exceeding the limit state gradually increases. After updating at 30 year, the exceeding samples are slightly reduced. Fig. 5 shows the result of the case with inspection rank I. Similarly samples for limit state 2 and 3 are shown in Fig. 6.

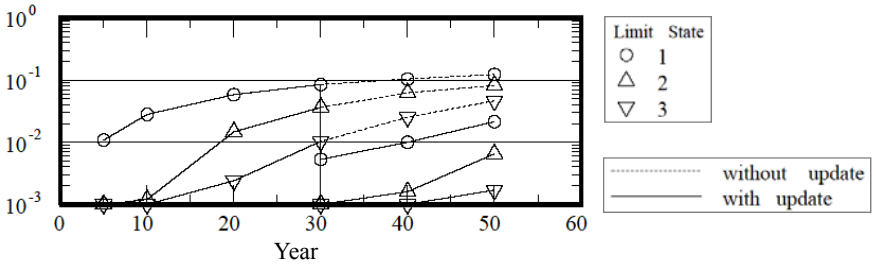

(1) Case 4 (visual inspection I + profile B)

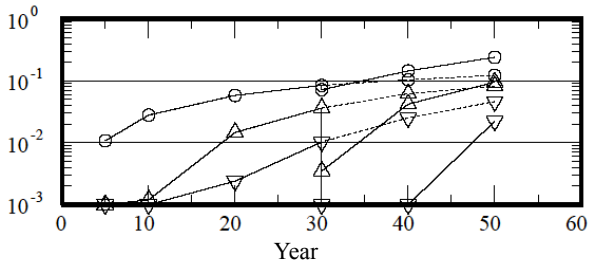

(2) Case 5 (visual inspection I + profile C)

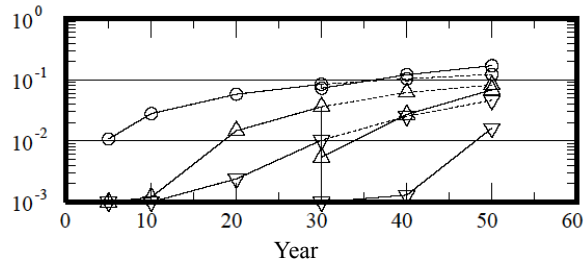

(3) Case 6 (visual inspection I + profile D)

Fig. 8 Three kinds of limit state probabilities over time

The limit state 2 indicates the initiation of concrete crack at surface, and the limit state 3 indicates the significant degradation of member strength. The limit state functions are constructed with respect to corrosion rate of rebar as shown in Eqs. (33) and (40). The samples are plotted in space of corrosion rate of rebar and the critical threshold value for the limit state 2 (crack initiation). Since the resistance value for the limit state 3 is given as deterministic value 20%, the limit state line is expressed by the horizontal broken line in the figure. The number of plotted samples in the figure is small at 5 year since samples exceeding the limit state 1 (initiation of rebar corrosion) are yet few. The samples exceeding the limit state 3 can be seen at 30 years before updating, however they vanish after the updating. Samples exceeding the limit state 2 are also reduced clearly.

Counting the number of samples exceeding the limit state, we can calculate the limit state probabilities. Figs. 7 and 8 show limit state probabilities over time, which are updated at 30 years after construction by visual inspection and chloride concentration profiling. The random variables of the model (Table 3) are updated by the assumed observation scenario in Table 6. Consequently the limit state probabilities are also updated based on them. Probabilities without any observation updating are calculated and shown in the figure for comparison.

In Case 1 which uses visual inspection rank I as observation data, the probabilities of all limit states are decreased after the observation updating. In Cases 2 and, 3, the probabilities are increased after the updating naturally since rank II, III means observation of crack on concrete surface. It is noted the probabilities can be updated though the information obtained by visual inspection is too small to identify model parameters. This difficulty in inverse or parameter identification problem is well known as ill-posedness or multicollinearity problem.

In addition to visual inspection result I, chloride concentrations through depth by coring test are considered as observation data in Case 4, 5 and 6. The assumed profiling is small in the sequence of A, B, C as shown in Figure 4. Naturally the updated probabilities are supposed to be large in the same sequence. Figs. 8(a) and (b) shows probabilities updated by profiling B (case 4) and C (case5). In both cases the probabilities are decreased by the updating at 30 years. The updated probabilities by profiling B is smaller than those by profiling C. Profile D has a special distribution that the chloride content is small near concrete surface, whereas large near rebar compared with profiling C. This difference of profiling suggests that the deterioration of the case with profiling D is more severe at just after the updating (30 years), however, in future less severe compared with the case of profiling C. Reflecting this feature, the limit state probabilities updated by profiling C is larger than those updated by profiling D at 30 year (just after updating), however the probabilities at 50 year (future) are smaller than those with profiling D.

5. Degeneracy in particle filter

Particle Filter (PF) has a problem known as degeneracy or sample impoverishment, which causes reduction of accuracy. In observation updating process by PF, the likelihood of each sample is estimated. The likelihood expresses the consistency between observed data and calculated data. The estimated likelihood of specific sample sometimes becomes very large especially when the assumed observation error (e.g., v in Eq. (41)) is small. In such a situation, accuracy of estimated probability is deteriorated significantly.

For the simplicity, only profiling of chloride concentrations by coring test is considered as observation data for numerical demonstration. It is assumed that observation is profile type C at 30

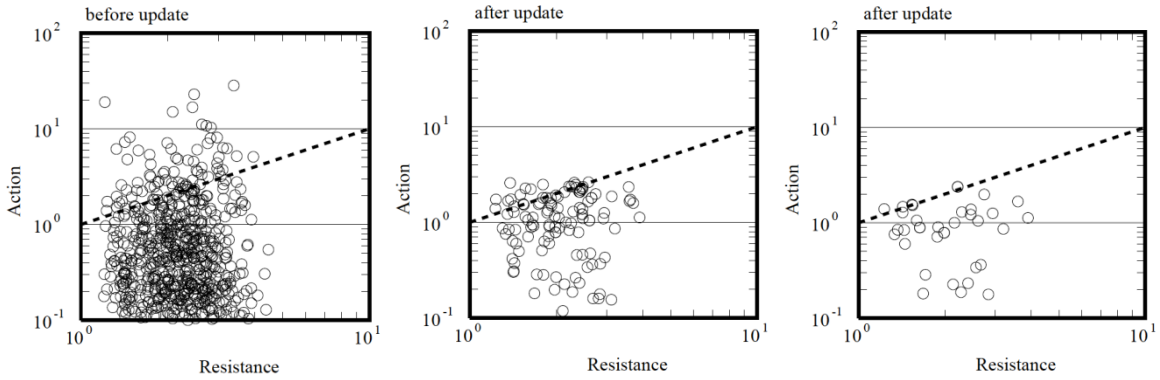

(1) Before updating (2) After updating, St. Dev. 1.0 (3) After updating, St. Dev. 0.5

Fig. 9 Distributions of resistance and action of limit state 1, updated by profile C at 30 years

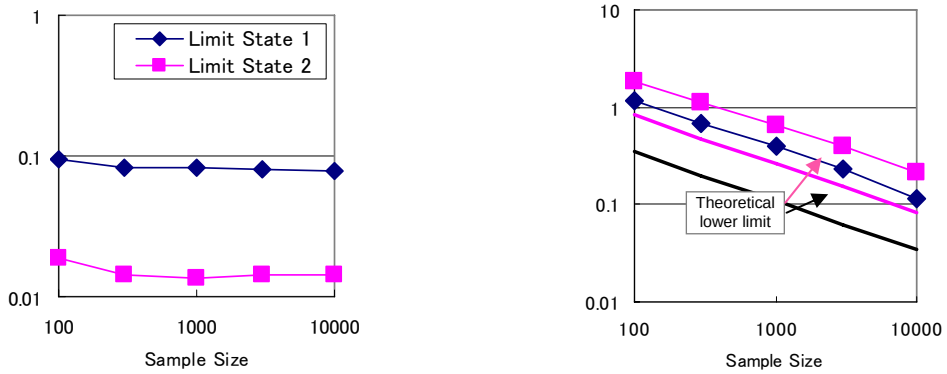

(1) Mean (2) COV

Fig. 10 Probabilities updated by Profile C; St.Dev. 1.0, Effective Sample Ratio 0.05

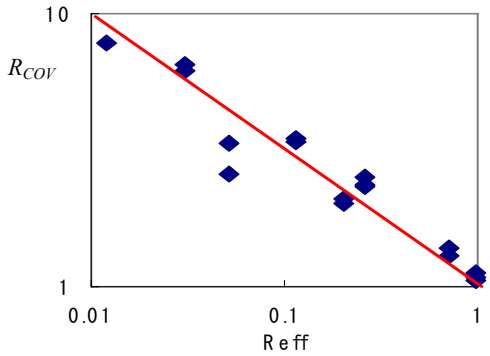

Fig. 11 Effective Sample Ration R_{eff} and R_{COV}; R_{COV}: Ratio to Theoretical lower limit COV

years and its standard deviation of the observation error is 1.0 or 0.5. Sample realizations of action and resistance of the limit state 1 at 30 years are shown in Fig. 9. The parameter for the limit state 1 is chloride concentration at rebar depth as shown in Eq. (28). The broken line in the figure indicates a limit state line for the initiation of rebar corrosion. The number of samples looks

fewer after the updating because of degeneracy in which samples with large likelihood is drawn many times and samples with small likelihood are discarded in the resampling process. Such a concentration or degeneracy is severe when the observation error is small, like the case with standard deviation 0.5 as shown in Fig. 9(c).

COV (Coefficient of Variance) of probability p calculated by ordinary MCS can be estimated by

$$COV = \sqrt{\frac{1-p}{np}} \tag{42}$$

where n is the number of sample in MCS. This equation is obtained assuming that each sample is perfectly independent. Eq. (42) indicates theoretical lower limit of COV of a probability calculated by PF. The degree of degeneracy can be estimated by following indicator, effective number N_{eff} (Ristic *et al*. 2004).

$$N_{eff} = \frac{1}{\sum_{i=1}^{n}\left(a_k^{(j)}\right)^2} \tag{43}$$

where $a_\nu^{(j)}$ is likelihood ratio. See Eq. (12). When likelihood of all samples are same, we have $a_k^{(j)} = 1/n$, consequently $N_{eff} = n$. When likelihood of one specific sample is 1.0 and those of the other are 0.0 as opposite extreme case, we have $N_{eff} = 1$. Effective sample ratio R_{eff} is introduced to discuss the accuracy of estimated probability.

$$R_{eff} = \frac{N_{eff}}{n} \tag{44}$$

In order to examine the accuracy depending on the degeneracy level R_{eff}, the calculation of probabilities updated by PF is repeated 100 times with different seed of random number. COV of estimated probabilities is calculated based on the 100 estimated probabilities. Sample size of SMCS is 100, 300, 1000, 3000 or 10000. Used observation is profile type-C and standard deviation of observation error is 1.0. Fig. 10 shows the mean and COV of probabilities obtained from the 100 simulations depending on the sample size. The mean is almost flat for sample size larger than 300. The lines of COV calculated by PF are parallel to the theoretical lower limit given by Eq. (42) but around three times larger than them. COV of probability obtained by 10000 sample case is 3.3 times larger than theoretical COV for limit state 1, while 2.6 times for limit state 2. Parameter R_{COV} that shows efficiency or accuracy is introduced and defined as ratio of obtained COV to the theoretical COV. The efficiency R_{COV} of limit state 1 and 2 are 3.3 and 2.6 respectively. The effective sample ratio R_{eff} in this simulation is 0.052. In the same way, we estimate COV when standard deviation of observation error is 2.0. The R_{COV} is 2.1 and 2.0 for limit state 1 and 2 respectively. The effective sample ratio R_{eff} is 0.20, which is larger than that of the case with observation error 1.0 because larger standard deviation makes the variation among likelihood of samples smaller relatively. Changing the standard deviation, type of observation, we obtained many sets of R_{eff} and R_{COV}, which are shown in Fig. 11. The obtained R_{COV} is almost proportional to effective sample ratio R_{eff} in logarithmic space. It indicates that we can predict accuracy level, namely, COV of probabilities calculated by PF, substituting effective number N_{eff} obtained by Eq. (43) into Eq. (42).

6. Conclusions

It is essential to update the model with reflecting observation or inspection data for reliability estimation of existing structures. The reliability estimation methodology by using Particle Filter (PF) are proposed and verified by hypothetical Gaussian linear model. It is also demonstrated through a numerical simulation on deteriorating RC structures due to chloride attack. Accuracy estimation is one of the important issues when Monte Carlo approach is adopted. Especially PF approach has a problem known as degeneracy. Effective sample size is introduced to predict the COV of limit state exceeding probabilities calculated by PF. The validity is shown by the numerical experiments.

There are several remaining future topics. Advanced Particle Filter is proposed to alleviate degeneracy problems. Merging Particle Filter (Nakano *et al*. 2007) is one of the advanced PF methods. It is simple but effective method to alleviate the degeneracy problem. This method conserves first and second moment of the original PDF. However, higher than second moment are not conserved. Though we examined the applicability of Merging Particle Filter to reliability estimation, the result is not good because probabilities are strongly influenced by tail part of PDF, which is sensitive to higher moment. The development of method that can alleviate the degeneracy and conserve the higher moment is one of the future topics.

As shown in this paper, modelling of observation error has strong influence on estimated probabilities. Modelling of spatial correlations of crack and chloride concentration are also one of the remaining problems. We need to accumulate the data of deteriorating structures for construction of more detailed stochastic model.

References

Akiyama, M., Frangopol, D.M. and Yoshida, I. (2010), "Time-dependent reliability analysis of existing RC structures in a marine environment using hazard associated with airborne chlorides", *Eng. Struct*., **32**(11), 3768-3779.

Alspach, D.L. and Sorensen, H.W. (1972), "Nonlinear Bayesian estimation using Gaussian sum approximations", *IEEE T. Autom. Contr*., **17**(4), 439-448.

Arulampalam, S., Maskell, S., Gordon N. and Clapp, T. (2002), "A tutorial on particle filters for on-line non-linear/non-Gaussian Bayesian tracking", *IEEE T. Signal Process*., **50**(20), 174-188.

Au, S.K. (2011), "Fast Bayesian FFT method for ambient modal identification with separated modes", *J. Eng. Mech*. ASCE, **137**(3), 214-226.

Ellingwood, B.R. (2005), "Risk-informed condition assessment of civil infrastructure: state of practice and research issues", *Struct. Infrastruct. E.*, **1**(1), 7-18.

Frangopol, D.M. (2009), *Life-cycle performance, management, and optimization of structural systems under uncertainty: accomplishments and challenges (Keynote paper)*, ICOSSAR, 38-60, Osaka, Japan.

Evensen, G. (1994), "Sequential data assimilation with a non-linear quasi-geostrophic model using Monte Carlo methods to forecast error statistics", *J. Geophys. Res*., **99**, 10143-10162.

Ge, L. and Soong T.T. (1998), "Damage identification through regularization method. I: theory", *J. Eng. Mech.- ASCE*, **124**(1), 103-108.

Gordon, N., Salmond, D. and Smith, A. (1993), "A novel approach to nonlinear / non-Gaussian Bayesian state estimation", *Proceedings of the IEEE on Radar and Signal Processing*.

Hoshiya, M. and Saito, E. (1984), "Structural identification by extended Kalman Filter", *J. Eng. Mech. -ASCE*, **110**(12), 1757-1770.

Honjo, Y., Wen-Tsung, L. and Sakajo, S. (1994), "Application of akaike information criterion statistics to geotechnical inverse analysis: the extended Bayesian method", *Struct*. *Saf*., **14**(1-2), 5-29.

Hoshiya, M. and Yoshida, I. (1996), "Identification of conditional stochastic Gaussian field", *J. EM.-ASCE*, **122**(2), 101-108.

Hoshiya, M. and Yoshida, I. (1998), "Process noise and optimum observation in conditional stochastic fields", *J. EM.-ASCE*, **124**(12), 1325-1330 .

Kitagawa, G. (1996), "Monte Carlo Filter and smoother for Non-Gaussian state space models", *J. Comput. Graph. Stat*., **5**(1), 1-25.

Julier, S.J. and Uhlmann, J.K. (1997), "A New Extension of the Kalman Filter to nonlinear Systems, Proceedings of AeroSense", *Proceedings of the 11th International Symposium on Aerospace/Defense Sensing*, *Simulation and Controls*, *Multi Sensor Fusion*, *Tracking and Resource Management II*, *SPIE*.

Nakano, S., Ueno, G. and Higuchi, H. (2007), "Merging particle filter for sequential data assimilation, *Nonlinear Proc. Geoph*., **14**(4), 395-408

Ristic, B., Arulampalam, S. and Gordon, N. (2004), *Beyond the Kalman Filter*, *Particle Filters for Tracking Applications*, Artech House.

Sato, T. and Kaji, K. (2000), "Adaptive Monte Carlo Filter and structure identification", *Proceedings of the first International Conference on Monte Carlo Simulation*, Monte Carlo, Monaco

Yoshida, I. and Sato, T. (2002), "Health monitoring algorithm by the Monte Carlo Filter based on non-Gaussian noise", *J. Nat*. *Disaster* Sci., **24**(2), 101-107.

Yoshida, I., Akiyama, M. and Suzuki, S. (2009), "Reliability analysis of an existing RC structure updated by inspection data", *Proceedings of the 10th International Conference on Structural Safety and Reliability*.

Yun, C.B. and Shinozuka, M. (1980), "Identification pf nonlinear structural dynamic systems", *J. Struct*. *Mech*.*-ASCE*, **8**(2), 187-203.